Contrib Mineral Petrol (1982) 79:368–374

Contributions to Mineralogy and Petrology

Phase Relationships in the System $KAlSiO_4-Mg_2SiO_4-SiO_2-H_2O$ as a Model for Hybridization Between Hydrous Siliceous Melts and Peridotite

Toshimori Sekine* and Peter J. Wyllie
Department of the Geophysical Sciences, University of Chicago, Chicago, Illinois 60637, USA

Abstract. The system $KAlSiO_4-Mg_2SiO_4-SiO_2-H_2O$ includes model representatives of (1) hydrous siliceous magma from subducted oceanic crust – the eutectic liquid in $KAlSi_3O_8-SiO_2-H_2O$, and (2) the overlying mantle peridotite – the assemblage forsterite + enstatite (Fo + En). In a series of partly schematic isobaric isothermal sections, the products of hybridization between the model materials at pressures between 20 and 30 kbar have been determined. The liquid dissolves peridotite components with little change in composition. Hybridization is not a simple mixing process, because of the incongruent melting of peridotitic assemblages with phlogopite (Ph). Hybridization causes solidification of the liquid, with products a sequence of three mineral assemblages: Ph, Ph + quartz (Qz), and Ph + En. The products represent an absolute geochemical separation and local concentration of all potassium from the liquid. Hybridization is accompanied by H_2O-saturation of melts, and evolution of aqueous fluid. Although there are significant differences between the melt composition and that of the magma rising from subducted oceanic slab, and between Fo + En and the mantle rock, extrapolation of the results suggests that the conclusions can probably be extended to mantle conditions with sodium in the melt, and jadeitic clinopyroxene included in the hybrid products.

Introduction

Nicholls and Ringwood (1973; reviewed by Ringwood 1975) developed a hypothesis in which hydrous siliceous melts (resembling rhyodacites), generated in the subducted oceanic crust, rose and reacted with the overlying peridotite. They proposed that the magmas would react to produce hybrid zones of olivine pyroxenite immediately above the oceanic slab, at depths of 100–150 km. Diapirs of olivine pyroxenite would rise episodically from this zone, and subsequent partial melting of these wet, hybrid rocks would produce a wide range of magmas, which may differentiate before eruption, with the most common composition being that of andesite. This is an attractive and versatile hypothesis, consistent with recent geochemical evidence in broad outline, but there are no experimental data supporting it in detail. What actually happens when hydrous siliceous melt from subducted oceanic crust reacts with mantle peridotite represents an enormous gap in our knowledge, filled at present by the simple assertion that olivine pyroxenite would be produced.

One way to investigate the products of hybridization is to model the phase relationships in synthetic silicate systems. Simple systems may illustrate the detailed mechanisms involved in natural hybridization processes in a way that is impossible in multi-component rock-mixing studies (which we also have under way). The system $MgO-SiO_2-H_2O$ is the simplest containing compositions representing peridotite (forsterite + enstatite) and hydrous siliceous liquid (eutectic between enstatite and quartz). Hybridization in this system between low-temperature siliceous liquid and the peridotite assemblage would certainly be dominated by the precipitation of enstatite, representing a pyroxenite. In this contribution, we explore the effect of one additional component, $KAlSiO_4$, and discover that the incongruent melting reactions involving phlogopite produce a series of hybridization products including phlogopite, and phlogopite ± enstatite ± quartz. The early hybridization process involves the extraction of all potassium from the liquid, with the precipitation of phlogopite.

The System $KAlSiO_4-Mg_2SiO_4-SiO_2-H_2O$

The H_2O-saturated liquidus surface for the system $Mg_2SiO_4-KAlSiO_4-SiO_2$ at 20 kb is illustrated in Fig. 1. Liquidus fields for forsterite (Fo), enstatite (En) and quartz (Qz) extend from the side $Mg_2SiO_4-SiO_2$ until they meet liquidus fields for phlogopite (Ph) and sanidine (Or). The field boundary between sanidine and quartz extending from the low-temperature eutectic on the side $KAlSiO_4-SiO_2$ terminates a very short distance into the system at the quaternary eutectic reaction:

$$\text{phlogopite} + \text{sanidine} + \text{quartz} + \text{vapor (V)} = \text{liquid (L)} \qquad (R_1)$$

at 680° C. The low-temperature liquids occupy a limited area close to the side $KAlSiO_4-SiO_2$. The liquidus surface for phlogopite rises steeply from the eutectic and the boundaries limiting the fields for sanidine and quartz.

The other two isobaric invariant liquid points are peritectics, representing incongruent melting reactions:

$$\text{phlogopite} + \text{quartz} + \text{vapor} = \text{enstatite} + \text{liquid} \qquad (R_2)$$

at 750° C, and:

Reprint requests to: P.J. Wyllie

* *Present address:* Department of Earth Sciences, Monash University, Clayton, Victoria 3168, Australia

0010-7999/82/0079/0368/$01.40

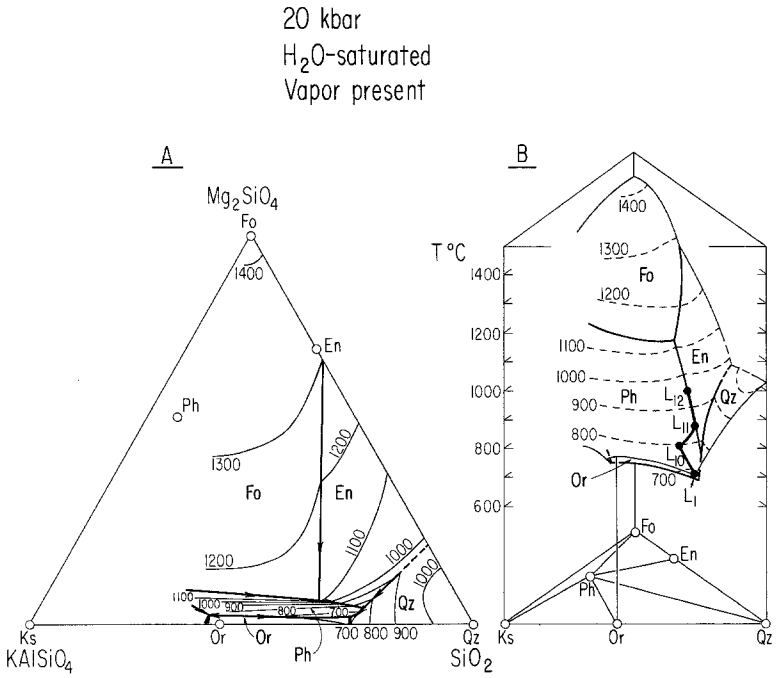

Fig. 1 A, B. H_2O-saturated liquidus for part of the system $KAlSiO_4-Mg_2SiO_4-SiO_2-H_2O$ at 20 kbar, based on available experimental data.
A Projection onto the system $KAlSiO_4-Mg_2SiO_4-SiO_4-SiO_2$ from H_2O apex, following Yoder (1976, p. 39), using experimental data from the systems $Mg_2SiO_4-SiO_2-H_2O$ (Kushiro 1969), $MgSiO_3-H_2O$ (Kushiro et al. 1968; Eggler 1973), $KMg_3AlSi_3O_{11}-H_2O$ (Yoder and Kushiro 1969; Wendlandt and Eggler 1980), $KMg_3AlSi_3O_{10}(OH)_2-MgSiO_3-H_2O$ (Modreski and Boettcher 1972). $KAlSi_3O_8-SiO_2-H_2O$ (Huang and Wyllie 1975) and from extrapolation of the low-pressure data in the system $KAlSiO_4-Mg_2SiO_4-SiO_2-H_2O$ by Luth (1967), given in Fig. 2. For graphical convenience, the liquidus surface is extended to SiO_2, despite the fact that SiO_2-H_2O is above its second critical end-point at 20 kbar (Kennedy et al. 1962; Nakamura and Kushiro 1974).
B T−X prism illustrating the shape of the liquidus surface. The path $L_1-L_{10}-L_{11}-L_{12}$ is described later in the text. Abbreviations: *Ks*, kalsilite; *Fo*, forsterite; *Qz*, quartz; *En*, enstatite; *Or*, sanidine; *Ph*, phlogopite

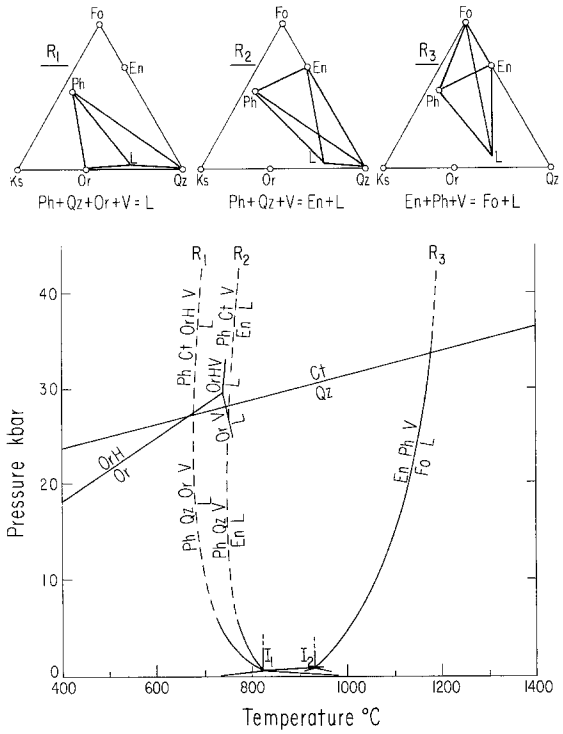

Fig. 2. Three univariant melting reactions in the system $KAlSiO_4-Mg_2SiO_4-SiO_2-H_2O$. Invariant points I_1 and I_2 are located near 0.5 kbar and 825° C where Ph, Qz, En, Or, and L coexist with aqueous vapor, and near 0.7 kbar and 930° C where Ph, En, Fo, Or, and L coexist with aqueous vapor (Luth 1967). The curve for the melting of Ph + En + V is from Modreski and Boettcher (1972). The other two estimated curves for the melting of Ph + Qz + Or + V and Ph + Qz + V are extrapolated to high pressures from the low pressure results of Luth (1967), using temperature values from Fig. 1 as controls. Univariant curves of Huang and Wyllie (1975) for Qz = Ct, Or + V = OrH, Or + V = L, and OrH + V = L are also shown. Tie-figures for the univariant reactions R_1, R_2, and R_3 with vapor omitted are depicted as projections from H_2O. Abbreviations: see Fig. 1; *Ct*, coesite; *OrH*, sanidine hydrate; *L*, liquid; *V*, vapor

phlogopite + enstatite + vapor
= forsterite + liquid (R_3)

at 1,130° C.

The tie-figures for reactions R_1, R_2, and R_3, projected from H_2O with the vapor omitted, are illustrated in Fig. 2, which also shows the univariant curves for these reactions, estimated through a range of pressures from sources cited in the legend. There is little variation in the temperatures of these three reactions through the pressure interval 20–30 kb.

The three reactions are represented by three subsolidus compatibility triangles, Ph−Or−Qz, En−Ph−Qz, and Fo−En−Ph (see Figs. 1B and 3F). Melting of each of these three mineral assemblages in the presence of H_2O at 20 kb produces liquid with compositions shown in Fig. 2 for reactions R_1, R_2, and R_3, respectively. Similarly, with crystallization of H_2O-saturated liquids with initial compositions in each of the three triangles, the liquids follow paths terminating at the corresponding isobaric invariant liquid point.

The phase volumes occurring beneath the liquidus surface are conveniently illustrated in two kinds of diagrams. Figure 3 shows a series of isobaric isothermal sections through the T−X prism of Figure 2B. The sections show phase fields, phase compositions, and the movement of three-phase triangles (four-phase figures if vapor were included) as temperature varies. Figure 4 shows three T−X sections, with the vertical edge T−Fo of the T−X prism (Fig. 1B) common to all of them. S_1, S_2, and S_3 are three mixtures of Or and Qz representing siliceous melts. The composition lines passing through S_1, S_2, and S_3 are drawn in Fig. 3F.

The isobaric isothermal sections in Fig. 3 illustrate the very restricted range of liquid compositions at low temperatures. Only at temperatures higher than that of R_3 does the liquid field expand significantly towards Mg_2SiO_4. Figure 3 also illustrates the successive loss of stable subsolidus joins with increasing temperature; Ph−Qz at R_2 between

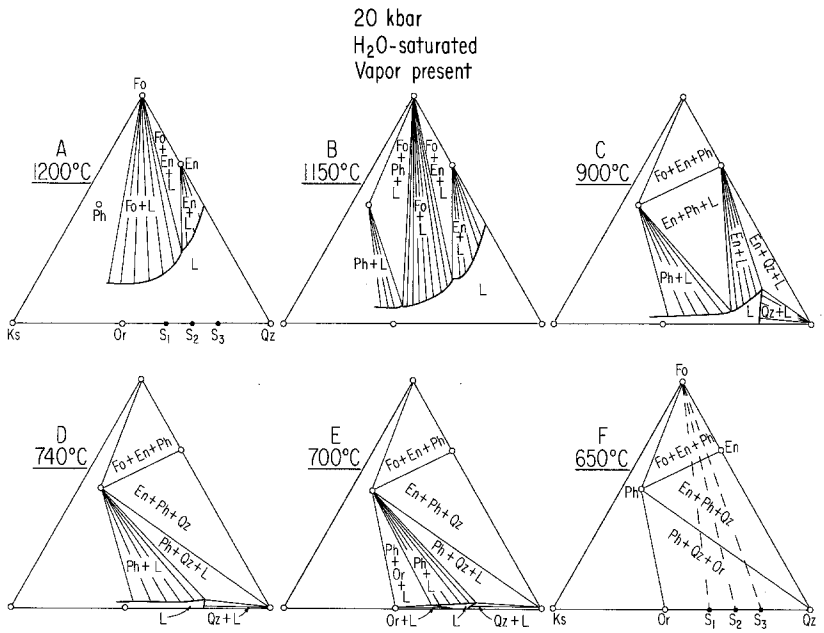

Fig. 3. Isobaric isothermal sections in the system $KAlSiO_4-Mg_2SiO_4-SiO_2-H_2O$ at 20 kbar constructed from Fig. 1A. Note that the tie-figures for R_1, R_2, and R_3 of Fig. 2 fit between these diagrams at 680° C, 750° C, and 1,130° C, respectively. Points S_1, S_2, and S_3 along the join Or–Qz correspond to 60Qz40Ks (by weight), 70Qz30Ks, and 80Qz20Ks. They represent compositions of siliceous melts. Abbreviations: see Fig. 1

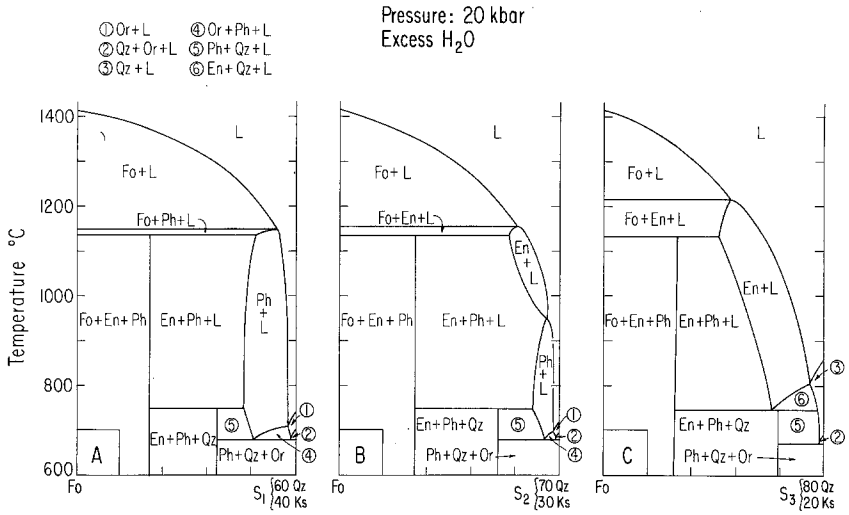

Fig. 4. Isobaric T–X sections for mixtures of Fo with S_1, S_2 and S_3 (Fig. 3F) in the system $KAlSiO_4-Mg_2SiO_4-SiO_2-H_2O$ at 20 kbar, based on Figs. 1 and 3. Abbreviations: see Fig. 1

Fig. 3D and C, and Ph–En at R_3 between Fig. 3C and B. Note that compositions in the triangle Fo–En–Ph remain crystalline through a wide range of temperatures, with the simultaneous existence of siliceous liquids occupying a restricted range of compositions close to the side Ks–Qz.

The isobaric T–X sections in Fig. 4 illustrate the equilibrium phase fields intersected by mixtures of Fo with the silicic compositions S_1, S_2, and S_3. Particularly noteworthy are the limited composition range of liquids through a wide temperature interval above the solidus near Ks–Qz, the wide extent of the fields for Ph+L and Ph+Qz+L, the increase in the size of the field for En+L with increasing Qz/Or, and the persistence of the assemblage Fo+En+Ph to higher temperatures than the other two subsolidus assemblages, En+Ph+Qz, and Ph+Or+Qz. The existence of crystalline Fo+En+Ph at the same temperatures as siliceous liquids is well displayed.

The lines Fo–S_1, Fo–S_2, and Fo–S_3 in Fig. 3 may be considered as mixing lines. The equilibrium phase assemblages produced by mixing and reacting Fo with the compositions S_1, S_2, and S_3 at any particular temperature can be read directly from the appropriate isothermal line in Fig. 4. Figure 3 is required to determine the compositions of the phases: the mineral compositions are defined, but the liquid compositions given by the corners of three-phase triangles or the ends of two-phase tie-lines vary considerably in directions transverse to the mixing lines, as shown by the liquidus field boundaries in Fig. 1.

Consider first the subsolidus mixing reactions (Fig. 3F). The mixing lines connecting assemblages of Or+Qz with Fo traverse three compatibility triangles and the two lines between them. As the bulk composition of any assemblage of Or+Qz is changed along any of these mixing lines, reaction with forsterite produces first phlogopite, until all of the sanidine is gone, then enstatite, until all of the quartz is gone, and the forsterite can then persist as a stable miner-

al. These reactions produce the sequence of phase assemblages: Ph + Or + Qz, Ph + Qz, En + Ph + Qz, En + Ph, and Fo + En + Ph. These phase fields are depicted in all three T − X sections below 680° C in Fig. 4.

The melting reaction (R_1) at 680° C terminates the subsolidus assemblage Ph + Or + Qz. Similarly, as shown in Fig. 4, the incongruent melting reactions R_2 and R_3 at 750° C and 1,130° C terminate the subsolidus assemblages En + Ph + Qz and Fo + En + Ph, respectively.

Figure 4 shows that, between 680° C and 750° C, addition of only a few per cent of Fo to molten or partially molten compositions S_1, S_2, and S_3 (assemblages L, L + Or, L + Qz, or L + Or + Qz) is sufficient to cause precipitation of phlogopite. There is a prominent phase field for Ph + L (Fig. 4A and B), and the field for Ph + Qz + L increases with increasing Qz/Or (Fig. 4A, B, and C). No enstatite is produced in equilibrium with liquid at temperatures below 750° C. Addition of Fo to the assemblage Ph + Qz + L continues reaction until all of the liquid is used up, producing Ph + Qz, and reaction with additional Fo causes the subsolidus changes described above, as illustrated in Fig. 3D, E, and F, as well as in Fig. 4.

The reaction R_2 at 750° C replaces the assemblage Ph + Qz + L with En + Ph + L (Fig. 4A and 4B), or En + Qz + L (Fig. 4C). However, the field for Ph + L is extensive above 750° C, with its upper temperature limit decreasing as the liquidus field boundaries between phlogopite-forsterite and enstatite-phlogopite decrease in temperature with increasing Qz/Or (Figs. 1 and 4).

At temperatures between 750° C and 1,130° C, the main sequences of phase assemblages produced by adding Fo to liquids with compositions S_1, S_2, and S_3 are L, En + L or Ph + L, or En + Ph + L. When the liquid is used up leaving the assemblage En + Ph, further addition of Fo produces the assemblage Fo + En + Ph without further reaction (compare Fig. 3C).

At temperatures above R_3 at 1,130° C, phlogopite can still be produced by reaction with liquids rich in Or/Qz (Figs. 3B and 4A), but for mixtures nearer to the eutectic composition in Or − Qz (Figs. 1, 3B, 4B and C), the sequence of phase assemblages is L, En + L, and Fo + En + L, or directly from L to Fo + L if the temperature is high enough (Figs. 3A and 4). At all temperatures below 1,130° C, the reaction of forsterite with siliceous liquid produces eventually a crystalline assemblage, but at higher temperatures the product is crystals plus liquid.

Hybridization Between Hydrous Siliceous Melt and Fo + En in the System $KAlSiO_4 - Mg_2SiO_4 - SiO_2$ at 20–30 kb

The phase relationships illustrated and described in Fig. 1 through 4 can be used to trace the precise sequence of reactions that would occur if a hydrous siliceous liquid with composition L_1 in Fig. 5 (the eutectic between sanidine and quartz) experienced hybridization with a crystalline assemblage P, representing peridotite (Fo + En with a trace of phlogopite).

The isothermal sections given in Fig. 5 are based on Figs. 1 and 3, with some expansion of the liquid fields for graphical clarity. The phase relationships for each isothermal section near the four temperatures listed probably vary little through the pressure range 20–30 kb (see Fig. 2). We are attempting to model reactions occurring as magmas

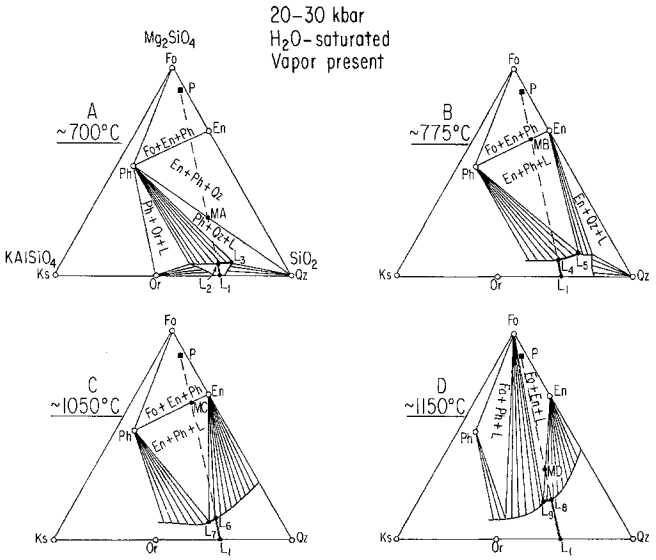

Fig. 5. Schematic isobaric isothermal sections in the system $KAlSiO_4 - Mg_2SiO_4 - SiO_2 - H_2O$, approximately applicable to any pressure from 20–30 kbar, based on Fig. 3. Note some expansion of the liquidus fields for graphical clarity. Points P and L_1 represent projections of peridotite and eutectic compositions in the join $Or - Qz - H_2O$, respectively. For derivation of the liquid paths from L_1, see text. Abbreviations: see Fig. 1

rise from subducted oceanic crust into overlying mantle wedge. The magmas rise from higher to lower pressures. The fact that pressure has little effect on the phase relationships through 20–30 kb permits us to use diagrams in Fig. 5 to illustrate polybaric isothermal processes.

The mantle wedge is hotter than the underlying subducted oceanic crust and the magmas generated from it. Therefore, the cooler magmas rise into hotter rocks. We can consider two limiting cases: (1) the hybridization reactions occur at the temperature of the magma, in which case we can use the isothermal section for that temperature, or (2) the low-temperature magma is heated to the temperature of the warmer host rock. Then we use an isothermal section at a higher temperature than the liquidus of L_1. For some more likely intermediate situation, where the reacting magma becomes hotter as it rises into the overlying mantle, we have to consider polythermal polybaric paths, which can be approximated by polythermal paths on the liquidus surface of the T − X prism in Fig. 1B (because this surface changes little through the pressure interval of the hybridization).

Low-Temperature Isothermal Hybridization

The H_2O-saturated eutectic for the system Or − Qz has composition L_1. Consider what happens when the low-temperature liquid L_1 comes into contact with crystalline peridotite, P, in Fig. 5A. The liquid dissolves a small amount of peridotite (Fo + En in proportion P), changing composition along the line L_1P. When its composition reaches L_2, phlogopite is precipitated. With continued addition of P at constant temperature, continued precipitation of phlogopite causes the liquid to change composition along the liquidus isotherm L_2L_3 as the bulk composition changes along the dashed line L_2P. At L_3, phlogopite is joined by quartz, and continued reaction of liquid L_3 with peridotite P causes

continued precipitation of phlogopite and quartz until all of the liquid is used up. If equilibrium is maintained, the original liquid L_1 is converted by hybridization to an assemblage of Ph + Qz, with bulk composition given by the point MA. After the liquid has disappeared, subsolidus reaction between Ph + Qz and the surrounding peridotite, Fo + En, generates zones of En + Ph + Qz, and En + Ph (Figs. 5A and 4B).

In the dynamic subduction zone environment, the crystalline products of hybridization may become separated from the reacting liquid. Under these circumstances, the products of hybridization would be a sequence of mineral assemblages: Ph, Ph + Qz, En + Ph + Qz, and En + Ph.

Intermediate-Temperature Isothermal Hybridization

Consider now what happens if the low-temperature eutectic liquid L_1 is heated to temperatures above that for reaction R_2 as it rises into the hotter peridotite. Figure 5B illustrates isothermal hybridization reactions under these circumstances. Liquid L_1 dissolves peridotite P until it reaches composition L_4, where precipitation of phlogopite begins. Continued reaction of the liquid causes precipitation of more phlogopite as the liquid changes from L_4 to L_5, while the bulk composition changes along the dashed line L_4P. Liquid L_5 precipitates enstatite and phlogopite until it is all used up. Under equilibrium conditions, the heated liquid L_1 is converted by hybridization to the assemblage En + Ph with bulk composition given by MB. In the dynamic subduction zone environment, separation of crystals and liquid would produce the mineral assemblages Ph, and En + Ph.

At somewhat higher temperatures, but below 1,130° C for reaction R_3, liquid L_1 dissolves more peridotite P, reaching composition L_6 in Fig. 5C. Addition of more P to liquid L_6 causes reaction of forsterite and precipitation of enstatite, causing the liquid to change direction along L_6L_7, which increase in the Ks component. When the liquid reaches L_7, enstatite is joined by phlogopite, and both are precipitated until all of the liquid is used up. The liquid L_1 is thus converted to the assemblage En + Ph with bulk composition given by MC. In the dynamic subduction zone environment, separation of crystals and liquid could produce the mineral assemblages En, and En + Ph.

High-Temperature Isothermal Hybridization

Figure 5D illustrates the reactions between partially melted peridotite P, and liquid L_1 superheated to temperatures above that of reaction R_3. The peridotite consists of Fo + En plus a trace of liquid L_9. We will assume for simplicity that the partially melted peridotite dissolves as a unit, P. Liquid L_1 dissolves a large amount of peridotite P (Fo + En + L_9) before it begins to precipitate enstatite when it reaches composition L_8. Continued precipitation of enstatite occurs, as the bulk composition follows the dashed line L_8-MD, and the liquid follows the path L_8L_9. The liquid L_9 coexists with forsterite and enstatite at constant temperature, so reaction ceases at this stage. The product of equilibrium hybridization between the heated liquid L_1 and crystalline peridotite is the liquid L_9 in equilibrium with a peridotite enriched in enstatite compared with the original peridotite, P. The original liquid L_1 is converted to a mixture of enstatite and liquid L_9 in the ratio L_9MD/MDEn. The original liquid L_9 in the partially melted peridotite is increased in amount, but with no change in composition. The assemblage does not crystallize completely as in the previous, low-temperature examples. However, early separation of crystals from liquid could produce a separate concentration of enstatite.

Polybaric-Polythermal Hybridization

We have concluded that the liquidus phase relationships change only slightly as a function of pressure between 20 and 30 kb and, therefore, let us assume that the isobaric T−X prism of Figure 1B is valid for the polybaric interval 20–30 kb.

Consider the low-temperature liquid L_1 at 700° C in Fig. 1B, rising from subducted oceanic crust to shallower levels, lower pressures, and higher temperatures. Assume that its temperature increases as it rises. It will dissolve the peridotite components, changing composition along the path L_1L_{10} which is sketched in space in Fig. 1B. When the liquid composition reaches the phlogopite liquidus surface at 800° C, precipitation of phlogopite proceeds as the liquid follows a path of increasing temperature across the liquidus surface, until it reaches the En−Ph liquidus field boundary at a point L_{11} at 850° C. Continued reaction with peridotite causes the liquid to precipitate En + Ph, and it follows the liquidus field boundary from L_{11} to higher temperatures as it continues to be heated. All of the liquid L_{12} is used up at 950° C, with consequences and products similar to those described for isothermal hybridization in Fig. 5B. The liquid path in Fig. 1B illustrates the wide range of depth-temperature conditions for the precipitation of phlogopite.

Liquid Composition During Hybridization

The siliceous liquid L_1 rising into peridotite P is constrained by the very steep liquidus surface to remain siliceous through a wide temperature interval (compare Figs. 1 and 5). The solution of peridotite components by the liquid does not lead to enrichment of the liquid in MgO, but to the precipitation of magnesian minerals. The forsterite of the peridotite is converted by the liquid into phlogopite, to the extent that there is K_2O available, and to enstatite. The liquid composition, once it reaches the liquidus surface for the magnesian minerals, changes in directions approximately perpendicular to the mixing line. The liquid may be enriched in SiO_2 or in $KAlSiO_4$, depending on whether phlogopite or enstatite is being precipitated, as shown in Fig. 5. When two or more minerals are being precipitated, the liquid path is given by the directions of field boundaries in Fig. 1. Because of the shape of the phlogopite liquidus surface, these paths are not directed towards significant enrichment in MgO until temperatures exceed reaction R_3 at 1,130° C, and the liquids coexist with both enstatite and forsterite.

Behavior of H_2O During Hybridization Reactions

We have considered the phase relationships for H_2O-saturated liquids, and assumed that this condition was not changed during the hybridization reactions. In fact, the progressive precipitation of minerals produced by the hybridization reactions does ensure that the liquids remain H_2O-

saturated. However, crystallization also requires that H_2O is progressively expelled during hybridization.

If the original siliceous liquids had been undersaturated with H_2O, the hybridization reactions at low- and medium-temperatures would produce H_2O-saturated liquids in the later stages of crystallization, before all of the liquid solidified. This would lead to the evolution of aqueous vapor.

Comparison of Model Materials with Subduction Materials

We can use the results described above as a model for the kind of reactions that may occur in the mantle wedge above a subducted oceanic crust, although we fully appreciate the fact that the melt composition differs significantly from that of magmas rising from the subducted crust, and the synthetic peridotite differs significantly from the mantle rock. The differences and their consequences for the analogy are considered below.

Peridotite

Peridotite in the model system, P in Fig. 4, consists of forsterite, enstatite and a trace of phlogopite. Peridotite in the mantle above the subducted oceanic crust is composed of olivine, orthopyroxene, clinopyroxene, and garnet (spinel at shallow levels), together with amphibole produced in its stability range, shallower than about 100 km, by aqueous fluids expelled from the subducted oceanic crust.

In the model system, it is the incongruent melting of assemblages involving phlogopite (reactions R_2 and R_3) which is responsible for the precipitation of phlogopite from the reacting siliceous liquid during hybridization. Modreski and Boettcher (1973) confirmed experimentally that phlogopite is involved in incongruent melting reactions in the presence of diopside as well as enstatite. They concluded that phlogopite peridotite in the mantle would similarly melt by incongruent reactions such as:

$$\text{phlogopite} + \text{orthopyroxene} + \text{clinopyroxene} = \text{forsterite} + \text{pyrope} + \text{liquid} \qquad (R_4)$$

and the analogous reaction in the presence of aqueous vapor. Incongruent melting reactions in phlogopite-peridotite have since been confirmed by Holloway and Eggler (1976) and by Wendtlandt and Eggler (1980). Therefore, we accept the working hypothesis that the behavior of phlogopite in the model system (Fig. 5) is a reasonable representation of its behavior in mantle peridotite-melt interactions.

Melt from Subducted Crust

According to Nicholls and Ringwood (1973), the liquid composition would be similar to that of rhyodacite. Values have been reported for measured and calculated liquid composition paths in a natural basalt, dry and with 5% H_2O at 30 kbar (Stern and Wyllie 1978), and for a model oceanic basalt in the system $CaO-MgO-Al_2O_3-SiO_2$ with 7.5% H_2O at 30 kbar (Sekine et al. 1981). The solidus temperatures for these samples at the stated conditions, recrystallized to quartz eclogites, are 760° C for the natural rock, and 810° C for the model composition. At 900° C the samples contain, respectively, about 20% and 15% H_2O-undersaturated liquid with composition richer in CaO/(CaO + MgO) than igneous rocks of the calc-alkaline series. The liquid in the natural rock contains 62.3% SiO_2, 22.7% Al_2O_3, 7.9% CaO, 2.5% (MgO + FeO), 3.6% Na_2O, and 0.7% K_2O (recalculated to 100% excluding H_2O). At temperatures nearer the solidus, the content of SiO_2 and alkalis would increase. However, the compositions of near-solidus liquids below 900° C have so far defied determination in both natural and synthetic systems.

The anhydrous composition of the H_2O-saturated liquid L_1 in Fig. 1B and 4, is 77.1% SiO_2, 11.9% Al_2O_3, 11.0% K_2O. The model liquid differs from the natural magma by the absence of (Ca + Fe + Mg), the absence of Na, and the much higher content of K. In terms of anticipated phase relationships, the absence of (Ca + Fe + Mg) is probably insignificant (except with respect to the compositions of the minerals produced during hybridization), the absence of Na is probably compensated for by the absence of diopside or clinopyroxene in the model peridotite (because in the natural system at the high pressures involved, one would expect the Na to become incorporated into clinopyroxene), and the higher content of K would increase the amount of phlogopite that could be produced.

Conclusion

Phase relationships in the model system $KAlSiO_4-Mg_2SiO_4-SiO_2-H_2O$ described above indicate that hybridization between hydrous siliceous melts and a simplified peridotite causes solution of the peridotite components with little change in liquid composition. Phlogopite is precipitated through a wide range of pressures, temperatures, and bulk compositions. Hybridization is not a simple mixing process. The process represents an absolute geochemical separation and local concentration of all potassium in the reacting system.

The precipitation of phlogopite-enstatite occurs for hybridization with all siliceous melts in the model system (Fig. 5), and this conclusion can probably be extended to phlogopite-orthopyroxene-clinopyroxene (with jadeite in solution), but this needs confirmation. The precipitation of phlogopite + quartz (or coesite) depends upon the melt composition remaining at sufficiently low temperature during hybridization (see Fig. 5). The precipitation of phlogopite alone will occur only if the liquidus field for phlogopite extends across the mixing line between the siliceous melt and the host peridotite (compare Figs. 4 and 5).

If the deduced reactions occur in the complex natural rock systems, with less potassium than in the synthetic system evaluated here, there are significant implications for the geochemistry of potassium, a key element in mantle metasomatism, magma generation, and development of the continental crust. These implications will be explored elsewhere (Wyllie and Sekine 1982).

Acknowledgements. This research was supported by the Earth Sciences Section of the National Science Foundation, NSF Grant EAR 76-20413 and NSF Grant EAR 81-08626.

References

Eggler DH (1973) Role of CO_2 in melting processes in the mantle. Carnegie Inst Washington Yearb 72:457–467

Holloway JR, Eggler DH (1976) Fluid-absent melting of peridotite containing phlogopite and dolomite. Carnegie Inst Washington Yearb 75:636–639

Huang W-L, Wyllie PJ (1975) Melting reactions in the system $NaAlSi_3O_8-KAlSi_3O_8-SiO_2$ to 35 kilobars, dry and with excess water. J Geol 83:737–748

Kennedy GC, Wasserburg GJ, Heard HC, Newton RC (1962) The upper three-phase region in the system SiO_2-H_2O. Am J Sci 260:501–521

Kushiro I (1969) The system forsterite-diopside-silica with and without water at high pressures. Am J Sci 267-A:269–294

Kushiro I, Yoder HS Jr, Nishikawa M (1968) Effect of water on the melting of enstatite. Geol Soc Am Bull 79:1685–1692

Luth WC (1967) Studies in the system $KAlSiO_4-Mg_2SiO_4-SiO_2-H_2O$: I, inferred phase relations and petrologic applications. J Petrol 8:372–416

Modreski PJ, Boettcher AL (1972) The stability of phlogopite and enstatite at high pressures: a model for micas in the interior of the earth. Am J Sci 272:852–869

Modreski PJ, Boettcher AL (1973) Phase relationships of phlogopite in the system $K_2O-MgO-CaO-Al_2O_3-SiO_2-H_2O$ to 35 kilobars: a better model for micas in the interior of the earth. Am J Sci 273:385–414

Nakamura Y, Kushiro I (1974) Composition of the gas phase in $Mg_2SiO_4-SiO_2-H_2O$ at 15 kbar. Carnegie Inst Washington Yearb 73:255–258

Nicholls IA, Ringwood AE (1973) Effect of water on olivine stability in tholeiites and production of silica-saturated magmas in the island arc environment. J Geol 81:285–300

Ringwood AE (1975) Composition and petrology of the earth, 618 p, McGraw-Hill, New York

Sekine T, Wyllie PJ, Baker DR (1981) Phase relationships at 30 kbar for quartz eclogite composition in $CaO-MgO-Al_2O_3-SiO_2-H_2O$ with implications for subduction zone magmas. Am Mineral 66:935–950

Stern CR, Wyllie PJ (1978) Phase compositions through crystallization intervals in basalt-andesite-H_2O at 30 kbar with implications for subduction zone magmas. Am Mineral 63:641–663

Wendlandt RF, Eggler DH (1980) The origins of potassic magmas: 2. stability of phlogopite in natural spinel lherzolite and in the system $KAlSiO_4-MgO-SiO_2-H_2O-CO_2$ at high pressures and high temperatures. Am J Sci 280:421–458

Yoder HS Jr (1976) Generation of basaltic magma, 265 p. Natl Acad Sci Washington DC

Yoder HS Jr, Kushiro I (1969) Melting of a hydrous phase: phlogopite. Am J Sci 267-A:558–582

Received, February 23, 1982; Accepted May 13, 1982